Structures of Biologically Active Oxysterols Determine Their Differential Effects on Phospholipid Membranes†

John B. Massey* and Henry J. Pownall

Section of Atherosclerosis and Lipoprotein Research, Department of Medicine, Baylor College of Medicine, One Baylor Plaza, Houston, Texas 77030

Received March 17, 2006; Revised Manuscript Received July 16, 2006

ABSTRACT: Oxysterols, derivatives of cholesterol that contain a second oxygen moiety, are intermediates in cholesterol catabolism, regulators of lipid metabolism, and toxic sterols with proatherogenic effects. In model membranes, cholesterol and eight selected oxysterols were compared by fluorescence probe techniques that measure changes in bilayer order and phase behavior and by the formation of detergent-resistant membranes (DRM). The oxysterols were modified on the sterol nucleus or on the isooctyl side chain. The model membranes consisted of dipalmitoyl phosphatidylcholine (DPPC) and mixtures of dioleoyl phosphatidylcholine with DPPC and with sphingomyelin. The different oxysterols induced changes in membrane properties according to the differences in their structures. Whereas the effects of some oxysterols on membrane order, fluorescence probe microenvironment, and DRM formation were similar to those of cholesterol, others had little or no effect. An empirical correlation ranking the oxysterols by their ability to modify membrane biophysical properties when compared to cholesterol led to a significant structure/function relationship between the biophysical measurements and an important cellular phenomenon, apoptosis. 7β-Hydroxycholesterol, which is the most cytotoxic of the eight selected oxysterols, was one of the least cholesterol-like with respect to modification of membrane properties. The results suggest that an underlying mechanism for oxysterol-induced apoptosis in cells, e.g., monocyte/macrophages, should include their biophysical effects on membranes, such as the regulation of the formation and composition of sterol-rich membrane domains.

Oxysterols are derivatives of cholesterol that contain a second oxygen atom as a carbonyl, hydroxyl, or epoxide group (*1*−*4*). Enzymatic oxidation of cholesterol occurs at various positions along the isooctyl side chain and at the 7α-position of the sterol nucleus. Enzymatically formed oxysterols are intermediates or end products in the biosynthesis of bile acids and steroid hormones and are signaling lipids that bind to nuclear liver X receptors (LXR)[1] (*1*) to activate gene transcription (*5*) and to oxysterol binding protein (OSBP)-related proteins to regulate cellular lipid metabolism and signal transduction (*2*, *6*, *7*). Nonenzymatic oxidations occur primarily on the sterol nucleus especially at the 7-position and at the 5,6-double bond. These oxysterols, which can be found in oxidized low-density lipoprotein (LDL) and in atherosclerotic lesions, can exert pathological effects such as induction of apoptosis (*8*−*22*). In smooth muscle cells, oxysterols may induce apoptosis by a mechanism that is similar to free cholesterol-induced cell death in macrophages (*11*). In macrophages, the accumulation of free cholesterol within endoplasmic reticulum (ER) membranes decreases bilayer fluidity, decreases the activities of integral membrane proteins [(e.g., sarco(endo)plasmic reticulum ATPase (SERCA)], and activates the unfolded protein response and other stress pathways that trigger apoptosis (*23*−*26*). However, in monocyte/macrophages, oxysterols induce apoptosis by mechanisms different than that of free cholesterol (*25*), which include a sustained increase in cytosolic free calcium (*12*−*14*), activation of calcium-dependent apoptotic and survival pathways (*12*−*20*), and induction of oxidative stress (*9*, *19*, *20*). 7-Ketocholesterol-induced increases in cellular calcium may involve changes in the lipid composition or biophysical properties of the plasma membrane which was suggested by the increased amount of the plasma membrane transient receptor potential calcium channel 1 in a detergent insoluble membrane fraction (*12*). Similarly, 7-ketocholesterol inhibition

† Supported by grants from the National Institutes of Health (HL-30914 and HL-56865 to HJP).

* Corresponding author at Section of Atherosclerosis and Lipoprotein Research, Department of Medicine, Baylor College of Medicine, The Methodist Hospital, MS A-601, 6565 Fannin Street, Houston, TX 77030. Phone: (713)798-4141. Fax: (713)798-4121. E-mail: jbm@bcm.tmc.edu.

[1] Abbreviations: ABCA1, ATP binding cassette transporter A1; ABCG1, ATP binding cassette transporter G1; ACAT, acyl-coenzyme A:cholesterol acyltransferase 1; apoA-I, apolipoprotein A-I; DMPC, dimyristoyl-*sn*-glycero-3-phosphocholine; DOPC, dioleoyl-*sn*-glycero-3-phosphocholine; DPH, 1,6-diphenyl-1,3,5-hexatriene; DPPC, dipalmitoyl-*sn*-glycero-3-phosphocholine; DRM, detergent-resistant membranes; EGF, epidermal growth factor; ER, endoplasmic reticulum; 5α-Epo, 5α,6α-epoxycholesterol; 5β-Epo, 5β,6β-epoxycholesterol; 7α-OH, 7α-hydroxycholesterol; 7β-OH, 7β-hydroxycholesterol; 20α-OH, 20-hydroxycholesterol; 22R-OH, 22R-hydroxycholesterol; 24α-OH, 24α-hydroxycholesterol; 25-OH, 25-hydroxycholesterol; 27-OH, 27-hydroxycholesterol; G.P., generalized polarization; HDL, high density lipoproteins; Laurdan, 6-dodecanoyl-2-dimethylaminonaphalene; L_d, liquid-disordered phase; L_o, liquid-ordered phase; LDL, low density lipoprotein; LXR, nuclear liver X receptors; MLV, multilamellar vesicles; PC, phosphatidylcholine; OSBP, oxysterol binding protein; SERCA, sarco(endo)plasmic reticulum ATPase; SM, sphingomyelin; T_M, midpoint temperature of the gel to L_d phase transition.

10.1021/bi060540u CCC: $33.50
Published on Web 08/09/2006

of apoliprotein A-I (apoA-I) mediated cholesterol efflux from macrophages was proposed to be due to its effect on the plasma membrane (*27*). The mechanisms by which oxysterols exert pathological effects are currently being determined to define the contribution of these lipids to the development of atherosclerosis. The effect of oxysterols on the biophysical properties of different cell membranes may be an important component of their pathological effects (*4*).

Cholesterol affects the function of membrane proteins through stereospecific ligand binding (*28*−*31*), through the induction of changes in the biophysical properties, e.g., fluidity, of membranes that affect protein conformation (*24*, *28*), and through the lateral segregation of proteins into microdomains which is determined by the preference of a protein for different types of lipid order (*26*, *32*−*34*). The interaction of cholesterol with saturated phosphatidylcholines and sphingomyelin facilitates the formation of the liquid-ordered (L_o) phase. In model membranes, the formation of phase-separated microdomains is dependent upon sterol chemical structure and leads to the classification of sterols that are "promoters" or "inhibitors" of the formation of ordered lipid domains (*35*−*44*). "Promoter" sterols also generally fit the definition of "membrane-active" sterols (*41*, *43*, *44*). Oxidative modifications of cholesterol generate sterols with different physicochemical properties and three-dimensional (3D) shapes. Oxysterols are less efficient than cholesterol at condensing or ordering fluid bilayers (*45*−*48*) and less hydrophobic where they can transfer between biological membranes at rates that are orders of magnitude faster than cholesterol (*49*−*51*). 7-Ketocholesterol can promote or inhibit the formation of ordered lipid phases depending upon the phospholipid composition (*29*, *48*). 25-Hydroxycholesterol can be a lipid-domain promoting sterol (*35*, *37*, *41*); however, it also can demonstrate anomalous behavior when compared to cholesterol (*43*, *46*, *52*, *53*). Cholesterol enhances the rate for the apoA-I-mediated microsolubilization of dimyristoyl-*sn*-glycero-3-phosphocholine (DMPC) multilamellar vesicles to form discoidal high-density lipoprotein (HDL) particles (*48*, *54*, *55*). The rate of DMPC microsolubilization is highly dependent upon the presence of lattice defects in the membrane surface that occur due to the imperfect packing of coexisting lipid phases. Some oxysterols are equally as efficient as cholesterol, whereas other oxysterols greatly inhibit this process (*48*, *55*). The probable basis for the differences among oxysterols is their differential ability to form L_o phases and induce lateral phase separation. On the basis of these results, oxysterols have different membrane biophysical properties based on the location and chemical nature of the oxygen substitution.

Sterols affect cellular processes by biochemical and membrane biophysical mechanisms. Structure/function studies comparing a series of sterols can be used to identify the mechanisms by which sterols regulate biological processes. This methodology has been used to investigate the role of cholesterol and other sterols in regulating receptor function (*28*) and in the regulation of proteins involved in cholesterol homeostasis (*29*−*31*). Oxysterols that are modified on the sterol nucleus are poor or ineffective ligands for LXR (*56*) and for sensing domains of cholesterol homeostatic proteins (*29*−*31*). The role of sterols in membrane-associated biochemical processes also can be studied by using e*nt*-cholesterol, which has cholesterol-like microdomain forming

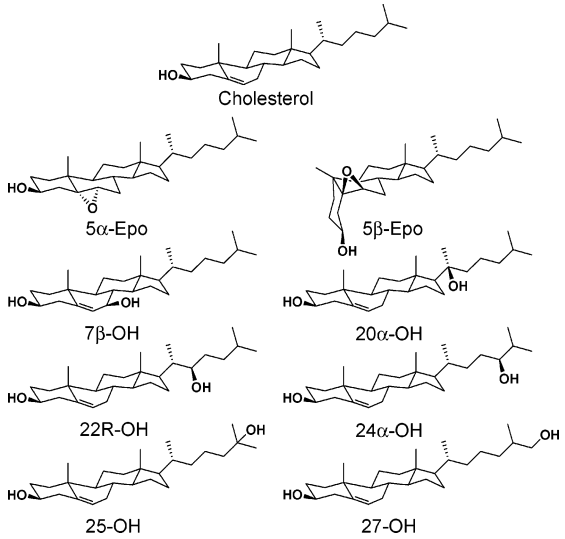

FIGURE 1: Structures of the sterols investigated in this study. Cholesterol, 5α,6α-epoxycholesterol (5α-Epo), 5*β*,6*β*-epoxycholesterol (5*β*-Epo), 7*β*-hydroxycholesterol (7*β*-OH), 20α-hydroxycholesterol (20α-OH), 22R-hydroxycholesterol (22R-OH), 24α-hydroxycholesterol (24α-OH), 25-hydroxycholesterol (25-OH), and 27-hydroxycholesterol (27-OH).

properties but does not interact with specific cholesterol-binding sites on proteins (*24*, *31*, *57*) and by systematically comparing "promoter" and "inhibitor" sterols to correlate changes in membrane physical properties with functional effects (*33*, *42*, *58*, *59*). Structure/function studies have demonstrated that oxysterols vary greatly in their ability to induce apoptosis and other physiological processes related to the progression of atherosclerosis (*8*−*10*). Of the most common oxysterols, 5*β*,6*β*-epoxycholesterol (5*β*-Epo), 7*β*-hydroxycholesterol (7*β*-OH), and 7-ketocholestrol are the most potent inducers of apoptosis. For this report, we chose a series of physiologically important oxysterols (Figure 1) for structure/function studies. 7*β*-OH, 5α,6α-epoxycholesterol (5α-Epo), and 5*β*-Epo occur in oxidized LDL, in human atherosclerotic lesions, and in the plasma of patients with stable coronary artery disease (*10*). 27-Hydroxycholesterol (27-OH) is the major oxysterol found in human atherosclerotic lesions and 24α-hydroxycholesterol (24α-OH) and 27-OH are the major oxysterols in human plasma. These sterols function in a form of reverse cholesterol transport where their formation is the first step in cholesterol catabolism and removal from the brain and atherosclerotic lesions, respectively (*1*). To a lesser extent, 25-hydroxycholesterol (25-OH) is also found in oxidized LDL and atherosclerotic lesions. 20-Hydroxycholesterol (20α-OH) and 22R-hydroxycholesterol (22R-OH) are intermediates in steroid hormone synthesis (*60*). 20α-OH, 22R-OH, 24α-OH, and 27-OH are ligands for the LXR nuclear receptors (*5*), and 25-OH binds to cytosolic binding proteins involved in signal transduction and membrane trafficking (*2*, *6*, *7*). Our results reveal that different oxysterols vary from being similar in magnitude to cholesterol in their effects on the biophysical properties of model membranes to those that demonstrate only small effects. 7*β*-OH would not induce the formation of an L_o phase and is an "inhibitor" sterol that would not form lipid rafts. According to an empirical correlation that compared the effects of oxysterols and cholesterol on membrane biophysical properties, there was a direct correlation between

the raft destabilizing tendencies of oxysterols and their induction of apoptosis in cells involved in atherosclerosis.

EXPERIMENTAL PROCEDURES

Materials. 5α,6α-Epoxycholesterol (cholestan-5α, 6α-epoxy-3β-ol), 5β,6β-epoxycholesterol (cholestan-5β, 6β-epoxy-3β-ol), 7β-hydroxycholesterol (5-cholesten-3β, 7β-diol), 20α-hydroxycholesterol (5-cholesten-3β, 20α-diol), 22R-hydroxycholesterol (5-cholesten-3β, 22(R)-diol), 24α-hydroxycholesterol (5-cholesten-3β, 24(S)-diol), 25-hydroxycholesterol (5-cholesten-3β, 25-diol), and 27-hydroxycholesterol (5-, 25R-cholesten-3β, 26-diol) were from Steraloids, Inc. (Newport, RI). Dipalmitoyl-*sn*-glycero-3-phosphocholine (DPPC), dioleoyl-*sn*-glycero-3-phosphocholine (DOPC), and porcine brain sphingomyelin (SM) were from Avanti Polar Lipids, Inc. (Alabaster, AL). 6-Dodecanoyl-2-dimethylaminonaphalene (Laurdan) and 1,6-diphenyl-1,3,5-hexatriene (DPH) were from Molecular Probes, Inc. (Eugene, OR). Cholesterol (5-cholesten-3β-ol) was from Sigma Chemical Co. (St. Louis, MO).

Liposome Preparation. The model membranes consisted of DPPC, DOPC/SM (3/2 mol/mol), and DOPC/DPPC (1/1 mol/mol) multilamellar vesicles (MLV). The appropriate amounts of phospholipids, sterols, and fluorescent probes were originally mixed in chloroform/methanol (2/1 v/v). The organic solvent was evaporated under a stream of nitrogen and the samples were lyophilized overnight. The dried lipids were dispersed in TBS buffer (100 mM NaCl, 10 mM Tris, 1 mM EDTA, 1 mM NaN_3, pH 7.4) by vortexing. To ensure complete hydration, the lipids were subjected to at least three freeze−thaw cycles that consisted of warming the samples to 50 °C, which was above the gel to liquid-disordered (L_d) phase transition of the highest melting phospholipids, and freezing the samples at −20 °C. For the fluorescence measurements, the probe to phospholipid molar ratio was 1/250 mol/mol.

Fluorescence Measurements. The fluorescence probes, DPH and Laurdan, were used to measure changes in the biophysical properties of model membranes. The polarization of DPH can be used to estimate the local "microviscosity" or molecular order in membranes (*48*, *61*, *62*). The fluorescence of Laurdan is dependent upon its microenvironment, which in membranes is dependent upon polarity and viscosity, and is highly sensitive to changes in lipid phases (*48*, *62*, *63*). Fluorescence measurements were performed on a Jobin Yvon Spex Fluorolog-3 FL3-22 spectrofluorimeter (Edison, NJ) that was equipped with Glan-Thompson polarizing prisms and a sample heater/cooler Peltier thermocouple drive. Fluorescence polarization measurements were performed as previously described (*48*, *54*, *62*). The fluorescence polarization of DPH was used to measure the effect of sterol structure on the acyl chain motion and phase properties of phospholipid bilayers. DPH partitions equally between gel, L_d, and L_o phases and thus does not preferentially monitor the behavior of one specific phase. The excitation wavelength was 350 nm, and the emission wavelength was 425 nm. Temperature-dependent measurements were collected in 1 °C increments; the samples were equilibrated for 1 min prior to each measurement. The instrument automatically measures the fluorescence polarization and corrects for the grating factor. The fluorescence emission spectra of the microenvironment sensitive probe, Laurdan, are highly dependent upon the phase state of the lipid matrix. Laurdan spectra demonstrate large blue shifts when the lipid matrix goes from an L_d to a gel state or upon the addition of cholesterol to an L_d phase bilayer (*54*, *62*, *63*). To facilitate the analysis of Laurdan fluorescence measurements, a normalization procedure, termed the general polarization (G.P.), was defined using two selective emission wavelengths (*63*). Fluorescence measurements were collected with an excitation wavelength of 350 nm, and the emission intensity measurements were made at 430 (I_{430}) and 480 (I_{480}) nm. The fluorescence intensities were used to calculate the generalized polarization of Laurdan (G.P. $= (I_{430} - I_{480})/(I_{430} + I_{480})$) (*54*, *62*, *63*). Similar to DPH, this probe partitions equally between gel and L_d phases. Temperature-dependent measurements were collected in 1 °C increments; the samples were equilibrated for 1 min prior to each measurement.

DRM Solubilization Experiments. Phospholipids and sterols that form tightly packed, ordered lipid domains may be resistant to solubilization by Triton X-100 (*33*, *35*, *36*, *39*, *48*, *61*, *64*, *65*). Under the appropriate conditions, detergent insolubility methods can be used to estimate the relative ability of a series of sterols to form ordered lipid domains (*35*, *36*, *39*). In model membranes, such as those studied here, the ability of a sterol to stabilize detergent-insoluble domains can correlate with the ability of a sterol to from ordered domains as measured by methods avoiding detergent (*33*). The solubilization of multilamellar vesicles, which varied in phospholipid and sterol composition, by 1% Triton X-100 was determined essentially as described by London and co-workers (*35*). The turbidity of liposomal samples (500 nmol of phospholipid in 1 mL of TBS) was measured as the optical density (OD_{400}) at 400 nm (using a Cary 25 spectrophotometer). To each of the samples, 50 μL of 10% (w/v) Triton X-100/TBS was added. The samples were then mixed, incubated at room temperature (~23 °C) overnight, and then the optical density was measured again. The ΔOD_{400} change was calculated as the ratio of the optical density after the Triton X-100 incubation (not corrected for dilution with Triton X-100 solution) to the optical density before the addition of Triton X-100.

RESULTS

Fluorescence Studies on Oxysterols in DPPC Bilayers. The fluorescence properties of DPH and Laurdan were used to measure sterol-induced changes in the biophysical properties of model membranes. For DPPC MLV, the DPH fluorescence polarization decreases sharply at the midpoint temperature of the gel to L_d phase transition (T_M) ($T_M = 40.6$ °C for DPPC) where the phospholipid passes from the gel to the L_d phase (*66*) (Figure 2A). Below T_M, where DPPC is in a gel phase, addition of 30 mol % cholesterol decreases lipid order as indicated by a decrease in the fluorescence polarization values (Figure 2A). The reductions in lipid order by 5α-Epo, 5β-Epo (Figure 2A), 7β-OH, 20α-OH (Figure 2B), 25-OH, 27-OH, and cholesterol (Figure 2C) were similar; the effects of 22R-OH (Figure 2B) and 24α-OH (Figure 2C) were smaller. As revealed by the increase in fluorescence polarization, above T_M, cholesterol increases acyl chain order. All sterols, except 22R-OH (Figure 2B) and 24α-OH (Figure 2C) greatly increased acyl chain order.

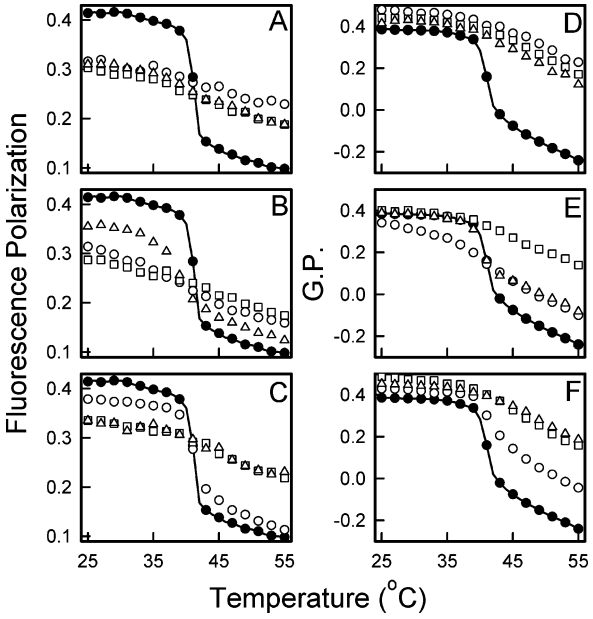

FIGURE 2: Effect of various sterols (30 mol %) on the DPH fluorescence polarization (A, B, C) and Laurdan G.P. (D, E, F) in DPPC MLV (0.1 mg/mL) as a function of temperature. (A, D) Chol (○), 5α-Epo (□), and 5β-Epo (△); (B, E) 7β-OH (○), 20α-OH (□), 22R-OH (△); (C, F) 24α-OH (○), 25-OH (□), and 27-OH (△). No sterol (●). For simplicity, only alternate data points are shown.

The Laurdan G.P. measurements also revealed that cholesterol (30 mol %) modulates changes in membrane properties associated with the phase transition of DPPC (Figure 2D). However, unlike DPH polarization measurements, the G.P. increased with addition of cholesterol below T_M (Figure 2D), and above T_M, cholesterol dramatically increased G.P. (Figure 2D); similar observations have been reported for cholesterol/SM bilayers (*62*). The G.P. versus temperature profiles of 5α-Epo, 5β-Epo (Figure 2D), 20α-OH (Figure 2E), 25-OH, and 27-OH (Figure 2F) were similar to that of cholesterol. However, the corresponding thermal profiles of 7β-OH, 22R-OH (Figure 2E), and 24α-OH (Figure 2F) were different. Above T_M, all three induced smaller increases in G.P. compared to sterol-free bilayers; 7β-OH also reduced G.P. below T_M.

The effect of sterol concentration on DPPC bilayers above (50 °C) and below (30 °C) T_M were determined by DPH fluorescence polarization and Laurdan G.P. measurements (Figure 3). At both temperatures, there was a linear correlation between the sterol concentration and the fluorescence measurements for each sterol. For simplicity, only the results for cholesterol and 7β-OH are shown in Figure 3. At 30 °C, both sterols induced identical linear decreases of DPH fluorescence polarization with sterol concentration, which demonstrates their equivalence in the disruption of the acyl chain packing of gel phase lipids (Figure 3A). As indicated by its greater slope (Δ*P*/mol %) (Figure 3A) at 50 °C, cholesterol clearly increased polarization more than 7β-OH. At 30 °C, cholesterol and 7β-OH, respectively, slightly increased and decreased the G.P. values with increasing sterol concentration (Figure 3B). However, at 50 °C, the effects of cholesterol on the slope (ΔGP/mol %) (Figure 3B) were much greater than those for 7β-OH. The slopes for the polarization (Δ*P*/mol %) and G.P. (ΔGP/mol %) indicate distinctive behavior by each sterol (Figure 4). Below T_M,

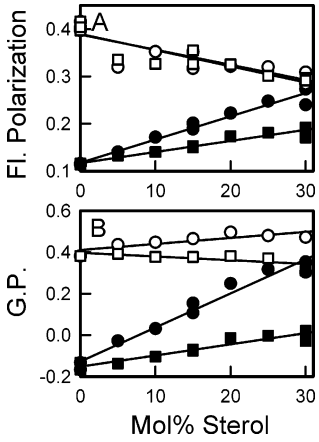

FIGURE 3: The DPH fluorescence polarization (A) and Laurdan G.P. (B) in DPPC MLV as a function of sterol concentration at 30 °C (○, □) and 50 °C (●, ■). Cholesterol (●, ○) and 7β-OH (■, □). The linear correlations typify all sterols studied. For simplicity, only the results for cholesterol and 7β-OH are shown.

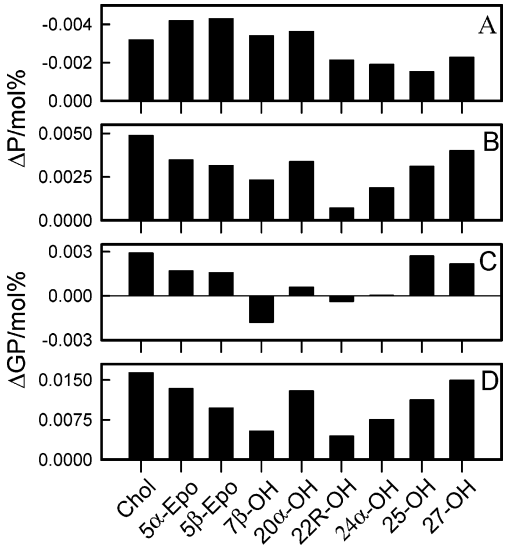

FIGURE 4: Slopes for the first-order line of regression correlating DPH fluorescence polarization and Laurdan G.P. with the sterol concentration in DPPC MLV. (A, B) Δ*P*/mol % sterol; (C, D) (GP/mol % sterol); (A, C) (30 °C) and (B, D) (50 °C).

sterols modified on the sterol nucleus have a greater change in Δ*P*/mol % than do the side chain-modified sterols (Figure 4A). However, this was not the case for the ΔGP/mol %; the values for 25-OH and 27-OH were equal to those found with cholesterol (Figure 4C). Above T_M, cholesterol was the most effective membrane-modifying sterol with the highest values for Δ*P*/mol % (Figure 4B) and ΔGP/mol % (Figure 4D). However, the different oxysterols vary from those having a small effect (e.g., 22R-OH) to those having effects similar to those of cholesterol (e.g., 27-OH).

Fluorescence Studies of Oxysterols in DOPC/SM and DOPC/DPPC Bilayers. Unlike binary cholesterol/DPPC mixtures, ternary mixtures of cholesterol with DOPC/SM and with DOPC/DPPC undergo micron-scale liquid−liquid-phase separation and have been used to directly observe membrane microdomain formation (*67*−*69*). The low polarization of DPH fluorescence in sterol-free DOPC/SM bilayers and its small temperature dependence (Figure 5) are consistent with these phospholipids forming one fluid phase (*61*−*63*). In DOPC/SM MLV containing the different sterols (30 mol %),

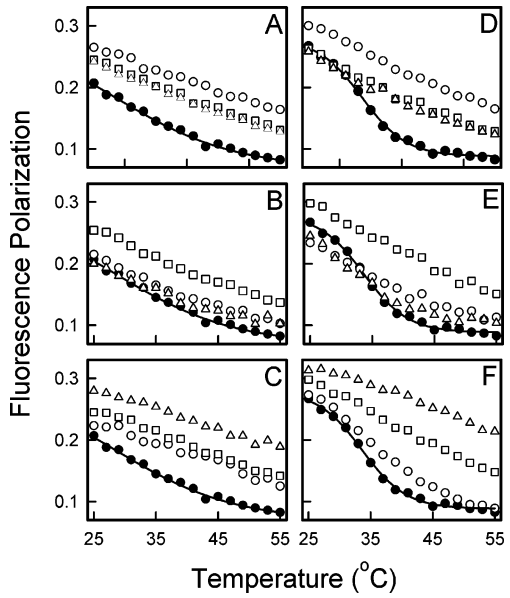

FIGURE 5: Effect of cholesterol and different oxysterols on the DPH fluorescence polarization in DOPC/SM (3/2 mol/mol) (A, B, C) and in DOPC/DPPC (1/1 mol/mol) (D, E, F) MLV as a function of temperature. The sterols (30 mol %) were Chol (○), 5α-Epo (□), and 5*β*-Epo (△) in A, D; 7*β*-OH (○), 20α-OH (□), and 22R-OH (△) in B, E; 24α-OH (○), 25-OH (□), and 27-OH (△) in C, F. No added sterol (●). Only every other temperature measurement is shown.

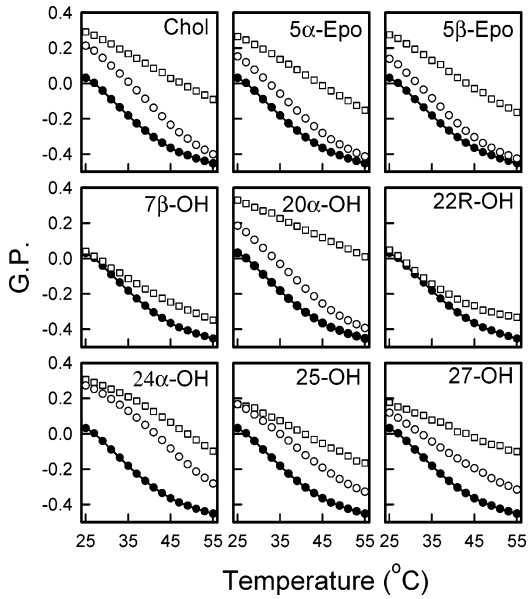

FIGURE 6: Effect of cholesterol and the different oxysterols on Laurdan G.P. in DOPC/SM (3/2 mol/mol) MLV as a function of temperature. The specific sterol studied is denoted in each panel. No added sterol (●); 5 mol % (○) and 30 mol % (□). Only every other temperature measurement is shown.

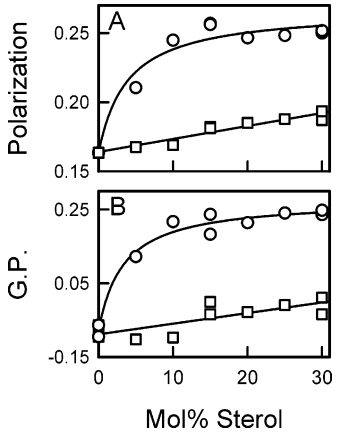

FIGURE 7: The DPH fluorescence polarization (A) and Laurdan G.P. (B) of DOPC/SM (3/2 mol/mol) MLV at 30 °C as a function of sterol concentration. Cholesterol (○) and 7*β*-OH (□). The data for cholesterol were fitted to the hyperbolic function, $y = y_o + ax/(b + x)$, and the data for 7*β*-OH (○) by linear regression. Similar measurements at 50 °C were linear (data not shown).

the DPH fluorescence polarization decreased essentially linearly with temperature (Figure 5). Relative to sterol-free bilayers, cholesterol increased the polarization of DPH fluorescence more than 5α-Epo, 5*β*-Epo (Figure 5A), 20-OH (Figure 5B), 24α-OH, and 25-OH (Figure 5C). However, the addition of 7*β*-OH and 22R-OH had only a small effect on the polarization (Figure 5B). 27-OH (Figure 5C) and cholesterol had nearly equal effects on the polarization of DPH fluorescence. As evidenced by the sigmoidal nature of a plot of DPH fluorescence polarization vs temperature, sterol-free DOPC/DPPC bilayers exhibit gel−liquid immiscibility; this was eliminated by addition of sterol (30 mol %) (Figure 5D). Cholesterol (Figure 5D), 20α-OH (Figure 5E), and 27-OH (Figure 5F) dramatically increased the polarization of DPH fluorescence, whereas 5α-Epo and 5*β*-Epo (Figure 5D) and 25-OH (Figure 5F) induced a moderate increase in polarization, and 7*β*-OH and 22R-OH (Figure 5E) and 24α-OH (Figure 5F) had only a small effect. Steady-state polarization measures the additive properties of the probe in different membrane domains that have different fluidities. In both phospholipid mixtures, there were prominent differences in the effects of the various sterols on acyl chain order, an effect that must be related to their different capacities to form ordered membrane domains. 25-OH and 27-OH behave distinctively in DOPC/SM and DOPC/DPPC mixtures (Figure 5), whereas in DPPC bilayers (Figure 2) their behavior is essentially identical.

In DOPC/SM and DOPC/DPPC bilayers, both the DPH polarization and G.P. vs temperature profiles are dose dependent with respect to sterol concentration. In DOPC/SM bilayers, the G.P. values at 25 °C were similar for 5 and 30 mol % cholesterol. However, at 55 °C there was a large difference (Figure 6). Similar sterol concentration dependences in the G.P. vs temperature profiles were found for 5α-Epo, 5*β*-Epo, 20α-OH, 24α-OH, 25-OH, and 27-OH. However, 7*β*-OH and 22R-OH induced only a small effect on G.P. compared to sterol-free bilayers. Previous studies have demonstrated that DOPC/SM/cholesterol and DOPC/DPPC/cholesterol bilayers undergo a transition from a system with two coexisting phases to a one-phase region over the temperature range studied (*67*−*69*). At 30 °C, DPH polarization and Laurdan G.P. were saturated with respect to cholesterol content in DOPC/SM bilayers (Figure 7A,B); above 10 mol % sterol, there was little additional change in the DPH polarization and G.P. measurements. At this temperature, this lipid system comprises two coexisting phases. These results are distinct from similar measurements in DPPC bilayers where linearity was observed with respect to sterol concentration in both gel and L_d phases (Figure 3). For both 7*β*-OH, DPH polarization and G.P. were linear with respect to sterol concentration (Figure 7A,B), and only a small increase was observed at maximum sterol levels (30

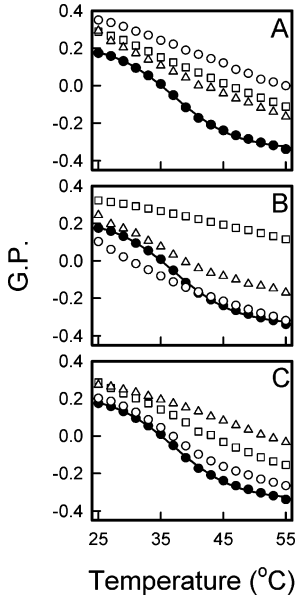

FIGURE 8: The effect of cholesterol and the different oxysterols (30 mol %) on Laurdan G.P. in DOPC/DPPC (1/1 mol/mol) MLV as a function of temperature. (A) Chol (○), 5α-Epo (□), and 5β-Epo (△). (B) 7β-OH (○), 20α-OH (□), and 22R-OH (△). (C) 24α-OH (○), 25-OH (□), and 27-OH (△). (A−C) no added sterol (●). Only every other temperature measurement is shown.

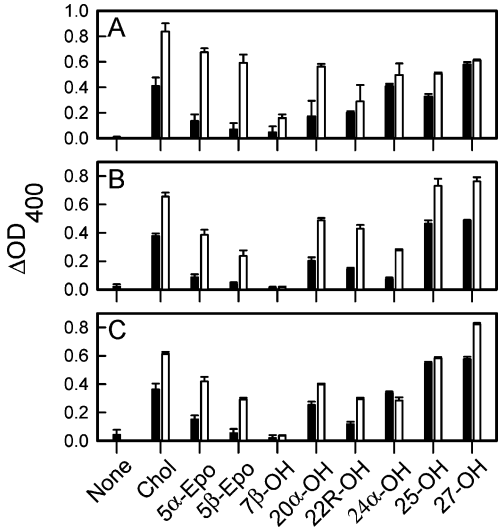

FIGURE 9: Effect of different sterols in MLVs on the formation of DRMs by Triton X-100 solubilization. (A) DPPC; (B) DOPC/DPPC (1/1 mol/mol); (C) DOPC/SM (3/2 mol/mol). Filled bars, 15 mol % sterol; open bars, 30 mol % sterol. Samples were measured in triplicate and are presented as the mean ± the standard error.

mol %). Similar to cholesterol, the effects of increasing concentrations of 5α-Epo, 5β-Epo, 20α-OH, 24α-OH, 25-OH, and 27-OH demonstrated saturation behavior where the maximum polarization and G.P. values were a function of the identity of the sterol (data not shown). 22R-OH demonstrated a similar behavior to 7-OH. However, at 50 °C, where the DOPC/SM/cholesterol system demonstrates one phase, the concentration dependences were mostly linear (data not shown) and similar to the results found with DPPC (Figure 3).

At 30 °C, the fluorescence polarization and G.P. measurements in DOPC/DPPC bilayers were also nonlinear with respect to sterol concentration (data not shown). In addition, each sterol (30 mol %) exhibited distinct G.P. vs temperature curves (Figure 8). Cholesterol (Figure 8A), 20α-OH (Figure 8B), and 27-OH (Figure 8C) dramatically increased G.P., whereas 5α-Epo, 5β-Epo (Figure 8B), and 25-OH (Figure 8C) produced moderate increases in G.P.; 7β-OH and 22R-OH (Figure 8B) and 24α-OH (Figure 8C) had only a small effect.

Effect of Oxysterols on Lipid Insolubility in Triton X-100. The Triton X-100-induced formation of DRMs in DPPC, DOPC/DPPC, and DOPC/SM bilayers was a function of the chemical structure of the oxysterol and of the sterol concentration (Figure 9). Bilayers containing 7β-OH did not form DRM under any of the conditions used; DRM formation in DPPC bilayers containing 25-OH, 27-OH, and cholesterol was similar. DRM formation in DOPC/DPPC and DOPC/SM bilayers containing 25-OH and 27-OH was equal to or greater than in those containing cholesterol. 5α-Epo and 5β-Epo induced less DRM formation than cholesterol, with 5α-Epo being more effective than 5β-Epo. DRM formation in bilayers containing the three other side chain modified sterols, 20α-OH, 22R-OH, and 24α-OH, was less than that observed in cholesterol-containing bilayers. However, the overall trend in each of the bilayer systems is that DRM formation in bilayers containing oxysterols was equal to that of cholesterol, less than that of cholesterol, or no DRM formation. This clearly demonstrates that the effect was due solely to the structure of the oxysterol.

Oxysterol Membrane Index. To establish a structure/function relationship between the membrane biophysics of oxysterols and a biological process, e.g., cell apoptosis, the DPH fluorescence polarization (Δ*P*/mol %, Figure 4B) and the Laurdan G.P. (ΔGP/mol %, Figure 4D) in DPPC bilayers at 50 °C, and DRM formation in DPPC bilayers containing 30 mol % sterol (Figure 9A) were used. For each of these measurements, cholesterol was the most effective sterol in modifying membrane properties. We defined an algorithm, termed the oxysterol membrane index (MI), in which each of the physical measurements were normalized to those of cholesterol using the following equation: $MI = 1 - [(M_{chol} - M_{sterol})/(M_{chol} - M_{low\ sterol})]$. M_{chol} and $M_{low\ sterol}$ are the values for a given membrane property of cholesterol and that of the oxysterol for which that property is lowest, and M_{sterol} is the corresponding membrane property for any given oxysterol. Thus, the MI values vary from 1 for cholesterol to 0 for the least effective oxysterol. According to the oxysterol MI, the oxysterols were ranked in descending numerical order (Figure 10A) where cholesterol > 27-OH > 5α-Epo > 25-OH > 5β-Epo > 24α-OH > 7β-OH > 22R-OH. The oxysterol MI also was compared for the sterols (30 mol %) in DOPC/SM and DOPC/DPPC bilayers. The results for DRM formation (Figure 10B), fluorescence polarization (Figure 10C), and G.P. (Figure 10D) were normalized and compared to the oxysterol MI. In general, there was a good correlation between the measurements in the more complex phospholipid mixtures and the oxysterol MI determined in DPPC bilayers. The exceptions were that bilayers containing 25-OH and 27-OH had higher ΔOD_{400}, 27-OH induced a higher polarization, and 20α-OH produced higher G.P. The ranking of the sterols by the oxysterol MI was consistent with their differential effects on membrane bilayer properties in both simple (e.g., DPPC) and complex (e.g., DOPC/SM) phospholipid systems.

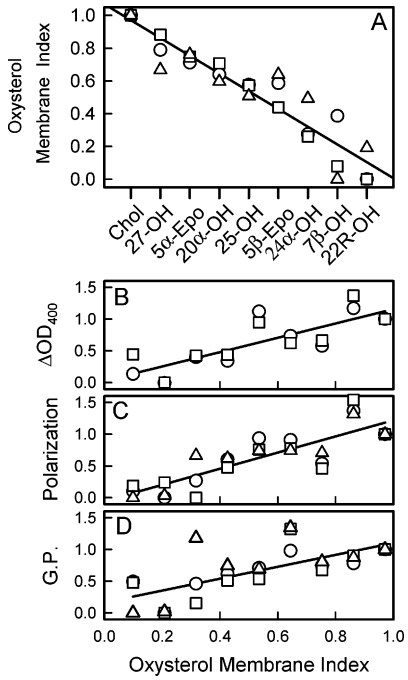

FIGURE 10: Comparison of the effects of different sterols on the membrane properties of MLV with different compositions. Data are normalized according to an oxysterol MI as defined in the text. (A) Rank order of the oxysterol MI for cholesterol and oxysterol properties in DPPC MLV as assessed by (○) DPH polarization (ΔP/mol %; from Figure 4B), (□) Laurdan G.P. (ΔGP/mol %; from Figure 4D), and (△) DRM formation at 30 mol % sterol (ΔOD_{400} from Figure 8A). The solid line represents the first-order line of regression ($r^2 = 0.88$) for a combination of the three sets of data (○, □, and △) versus the sterols position on the abscissa. The nine different sterols were assigned a number from 1 for cholesterol to 9 for 22R-OH for this calculation. (B, C, D) Comparison of oxysterol membrane index for DPPC MLV with those for DOPC/SM and DOPC/DPPC MLV, all with 30% mol sterol. (B) DRM formation (ΔOD_{400} from Figure 8) for DOPC/DPPC (○) and DOPC/SM (□). (C) DPH fluorescence polarization in DOPC/SM MLV at 30 °C (○) and 50 °C (□) and DOPC/DPPC MLV at 50 °C (△). (D) Laurdan G.P. in DOPC/SM MLV at 30 °C (○) and 50 °C (□) and DOPC/DPPC MLV at 50 °C (△). In B, C, and D the solid line represents the first-order line of regression.

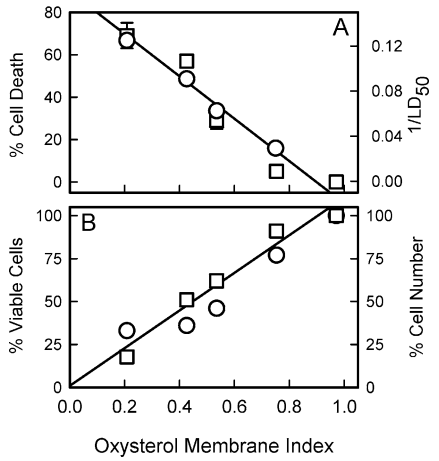

FIGURE 11: Comparison of the oxysterol membrane index with cell apoptosis induced by 5α-Epo, 5β-Epo, 7β-OH, and 25-OH. (A) Correlation of oxysterol MI with % cell death (□; $r^2 = 0.92$) and $1/LD_{50}$ (○; $r^2 = 0.99$) in human arterial endothelial cells (*10*). The solid line represents the linear regression analysis for the % cell death. (B) Correlation of membrane index with % cell number (□; $r^2 = 0.96$) and % viable cells (○; $r^2 = 0.93$) in human monocytic U937 cells (*8*). The solid line is the linear regression analysis for the % cell number.

Two studies have investigated the effects of oxysterol structure on an important biological process in atherosclerosis, i.e., apoptosis. 5α-Epo, 5β-Epo, 7β-OH, and 25-OH induced apoptosis was determined in human aortic endothelial cells (*8*) and the human monocytic U937 cell line (*10*). In endothelial cells, there was a linear correlation when the oxysterol MI was analyzed against the % cell death at one oxysterol concentration and $1/LD_{50}$ (LD_{50} is the oxysterol concentration where 50% of the cells were nonviable) (Figure 11A). In U937 cells, there was a linear correlation when the oxysterol MI was analyzed against the % viable cells and the % cell number (Figure 11B). The results indicate a direct correlation between the effect of oxysterols on membrane biophysical properties and their ability to induce cell apoptosis.

DISCUSSION

Oxysterols have many diverse biological activities related to cholesterol function and metabolism in normal and diseased states (*1*−*7*). They demonstrate a great deal of structural diversity due to the chemical nature of the oxygen moiety, its location on the parent cholesterol molecule, and its chirality. Of the oxysterols found in oxidized LDL and atherosclerotic lesions, 5β-Epo, 7β-OH, and 7-ketocholesterol are the most potent inducers of apoptosis in cultured cells (*8*−*10*). Because of the hydrophobic nature of oxysterols, they should have an equilibrium location within biological membranes. Cholesterol affects membrane structure by increasing bilayer thickness, decreasing membrane permeability, modulating acyl chain motion, decreasing interfacial hydration, and forming L_o microdomains. In model membranes, specific "promoter" sterols can induce liquid−liquid-phase separation, whereas others have little or no effect (*35*−*44*). Sphingolipid- and cholesterol-rich domains or rafts in the plasma membrane have been implicated in many biochemical processes (*26*, *32*−*34*); however, they also sequester unesterified cholesterol where non-raft cholesterol in the ER can have regulatory effects in normal cells (*70*, *71*) and toxic effects in cholesterol-loaded cells (*23*−*26*, *72*, *73*). We used techniques that measure lipid order, fluorescence probe microenvironment, and DRM formation to compare a series of oxysterols (Figure 1) with cholesterol. Our results indicate that the location of the oxygen moieties and their chiral nature determine the packing of oxysterols in phospholipid bilayers. The linear relationship between the oxysterol MI and cell apoptosis strongly support the concept that cytotoxic oxysterols elicit at least a part of their biological effect through alterations in membrane structure.

Oxysterols Modified on the Sterol Nucleus. 7β-OH is formed by nonenzymatic oxidation and is the most cytotoxic oxysterol found in oxidized LDL and atherosclerotic lesions (*8*−*10*, *24*, *17*−*20*). In DPPC bilayers, 7β-OH is less effective than cholesterol in modulating membrane properties as determined by polarization and G.P. measurements. Additionally, compared to cholesterol, it also induces smaller changes in membrane properties in DOPC/SM and DOPC/DPPC bilayers. 7β-OH did not form DRM in any of the phospholipid bilayers studied and had the second lowest oxysterol MI. Like 7-ketocholesterol and 6-ketocholestanol,

7β-OH may have a "tilted" sterol orientation to the lipid−water interface (*38*, *74*). The insertion of a polar oxygen moiety into the hydrophobic portion of the bilayer is thermodynamically unfavorable (*75*). Location of the 7β-hydroxyl at the lipid−water interface with the 3β-hydroxyl would be thermodynamically favorable and would tilt the sterol nucleus with respect to the bilayer plane so that it does not penetrate as far into the bilayer as cholesterol. Cholesterol extends ~6 Å further into the membrane bilayer than a tilted 6-ketocholestanol (*38*, *74*). The tilting of the sterol would be more readily accommodated in bilayers with loosely packed phospholipids with high molecular surface areas (e.g., DOPC) than with phospholipids that have small surfaces areas (e.g., DPPC) (*76*). Our results indicate that 7β-OH would not form the attractive van der Waals interactions needed for a tightly packed L_o phase and would preferentially partition into an L_d phase. In cells, whether 7-OH is primarily localized to the plasma membrane domains similar to cholesterol or is located in different cellular membranes is unknown.

5α-Epo and 5β-Epo, also formed by nonenzymatic oxidation, are found in oxidized LDL and atherosclerotic lesions. In cell studies, 5β-Epo is much more cytotoxic than 5α-Epo (*8*−*10*, *14*, *21*). The modulation of membrane biophysical properties by 5α-Epo and 5β-Epo was similar to that for cholesterol. However, they were not as effective as cholesterol, and 5α-Epo has a higher oxysterol MI than 5β-Epo. The location of the epoxy moiety at carbons 5 and 6 could change the orientation of the sterol nucleus to bring both of the oxygen moieties (i.e., 3β hydroxyl group) close the bilayer surface and also create a steric effect where its bulkiness reduces the interfacial packing with phospholipids. Models suggest that these diastereomers have different 3D shapes. 5α-Epo maintains the planarity of the A and B rings in the tetracylic ring system, similar to cholesterol, whereas 5β-Epo would be less planar (Figure 1). According to our results, 5α-Epo has tighter interactions with phospholipids than does 5β-Epo and would be considered a better raft-stabilizing sterol.

Oxysterols Modified on the Sterol Side Chain. 20α-OH, 22R-OH, 24α-OH, 25-OH, and 27-OH are formed enzymatically (*1*). 20α-OH regulates cholesterol and steroid hormone synthesis by post-translational and transcriptional mechanisms (*60*). Our studies indicate that 20α-OH closely mimics the membrane-modulating properties of cholesterol. This part of the side chain is probably rigid because of restrictions posed by C18 and C21 methyl groups. Similar to cholesterol, 20α-OH must maintain a wedge shape with a planar α-face and a bulky β-face.

Formation of 22R-OH is the first committed step in the conversion of cholesterol to steroid hormones; this oxysterol is a major activator of LXR (*5*). 22R-OH is similar to 7β-OH in that it does not induce increases in polarization and G.P. in DPPC, DOPC/SM, and DOPC/DPPC bilayers. However, it does induce DRM more effectively than does 7β-OH. 22R-OH ranked the lowest on the oxysterol MI. Earlier studies indicated that the poor interaction of 22R-OH with phospholipids was very stereospecific since 22S-OH and 22-ketocholesterol are much more effective modulators of bilayer properties (*45*). According to monolayer studies, 22R-OH could have two orientations in membranes. In one, the sterol nucleus lies parallel to the air−water interface where both hydroxyl groups are solvated; in the other it emulates cholesterol, in which the 3β hydroxyl is directed toward the interface and the sterol nucleus is perpendicular to the plane of the bilayer. In bilayers, 22R-OH has a kink (one additional *gauche* configuration) between the side chain and the long axis of the sterol nucleus that inhibits tight sterol−phospholipid association (*45*).

Our studies indicate that 25-OH and 27-OH form ordered lipid domains. In DOPC/SM and DOPC/DPPC, both were more effective than cholesterol at forming DRM. Similar results were previously found for 25-OH (*35*−*37*). These results suggest that these sterols have an "upright" orientation that is similar to that of cholesterol. L_o phase lipids have a greater membrane thickness than do L_d phase lipids. C18:0SM/cholesterol, DOPC, and DOPC/cholesterol bilayers have membrane thicknesses of 4.6, 3.5, and 4.0 nm, respectively (*32*). These sterols may partition more into ordered lipid phases, which are thicker, because their greater molecular length favors a larger number of energetically favorable hydrophobic matches with the phospholipid acyl chains. These results would suggest that these sterols would accumulate in sphingolipid-rich domains rafts in cells. However, they may not be restricted to these domains since both sterols spontaneously transfer between membranes at rates that are orders of magnitude faster than cholesterol (*50*, *51*). However, when compared to cholesterol, 25-OH and 27-OH exhibit anomalous behavior when mixed with POPC and DOPC. 25-OH and 27-OH induce an expansion and not a condensation of POPC monolayers (*53*), 25-OH increases the glucose permeability egg lecithin liposomes (*46*), and small-angle X-ray diffraction studies indicated that 25-OH does not intercalate into the membrane hydrocarbon core and is primarily associated with the hydrated surface of the bilayer (*52*). Monolayer studies indicate that at low surface pressures 25-OH and 27-OH have their sterol nucleus parallel to the air−water interface where both hydroxyl groups are solvated (*53*). However, 25-OH and 27-OH had limiting molecular areas smaller than that of cholesterol, which led to a model in which the side chain alcohol group is anchored at the interface giving these sterols an "inverse orientation" with respect to cholesterol (*53*). Sterols, which have side chains with a polar fluorescent or spin-label reporter group, also have been suggested to have an "inverse orientation" in a membrane (*77*). 25-OH and 27-OH could have three orientations in a bilayer based on how tightly they interact with the acyl chains of phospholipids. They can be oriented like cholesterol in L_o phases and have a surface location where both hydroxyls are hydrated or an "inverse orientation" in L_d phases. Similarly, in polyunsaturated phosphatidylcholine (PC) bilayers, cholesterol does not demonstrate an "upright" membrane orientation because of poor sterol−acyl chain interactions (*78*).

There have been no previous studies on the membrane behavior of 24α-OH. Our spectroscopic studies reveal membrane properties that are similar to those of 22R-OH in DPPC and DOPC/DPPC bilayers; in contrast, DRM formation was similar in all the bilayer systems studied. In DOPC/SM bilayers, the polarization and G.P. measurements for 24α-OH were similar to those for 25-OH. Formation of 24α-OH is the major mechanism for the elimination of cholesterol from the brain, and it also transfers rapidly between membrane surfaces and is rapidly eliminated from plasma

(*51*). The inability of 24α-OH and 22R-OH to form tightly packed sterol−phospholipid interactions and rapidly transfer between membranes may be important to their biological activity as regulatory sterols. A series of oxygenated sterols without an isooctyl side chain do not form ordered lipid domains, suggesting that the isooctyl side chain is essential to a domain forming sterol (*37*). However, our studies demonstrate that the stereochemistry of a functional oxygen moiety is a determinant of sterol orientation in membranes, sterol−phospholipid interactions, and domain formation.

Physiological Relevance. Oxysterol MI is an algorithm that allows the comparison of the effect of oxysterols on membrane biophysical properties with each other and with that of a measured biological phenomenon. Even though there were some differences for the oxysterols in different bilayer systems, a general trend held for all of the sterols studied (Figure 10). Using data on oxysterol-induced apoptosis in human aortic endothelial cells and a monocytic U937 cell line, there was a direct correlation between the effects of specific oxysterols on membrane biophysical properties and their ability to induce cell apoptosis (Figure 11). 5α-Epo, 5β-Epo, 7β-OH, 7α-OH, 7-ketocholesterol, 25-OH, and 27-OH induce apoptosis in cells albeit with different efficacies (*8*−*10*). The β-isomers, 5β-Epo and 7β-OH, are more potent inducers of apoptosis than the corresponding α-isomers, 5α-Epo and 7α-OH (*8*−*10*). 7β-OH, 25-OH, and 7-ketocholesterol induce apoptosis in smooth muscle cells (*11*) and in monocyte/macrophages and endothelial cells by different mechanisms (*8*−*10*, *12*−*19*). In smooth muscle cells, apoptosis may be induced by an ER-dependent mechanism (*11*) and in monocyte/macrophages by a calcium-dependent mechanism that may involve plasma membrane domains (*12*). In monocytic cells, there was no relationship between oxysterol-induced cytotoxicity and HMG-CoA reductase activity (*9*), which indicates that inhibition of isoprenoid-based cholesterol biosynthesis (*79*) is not involved. Our results indicate that the membrane biophysical properties of specific unesterified oxysterols determine their cellular function.

In normolipidemic cells, most unesterified cholesterol is in the plasma membrane where cholesterol levels are tightly maintained by homeostatic mechanisms. In cholesterol-loaded cells, the amount of free cholesterol is also determined by the action of ATP binding cassette transporter A1 (ABCA1), ATP binding cassette transporter G1 (ABCG1), and acyl-coenzyme A:cholesterol acyltransferase 1 (ACAT) (*26*, *80*). ABCA1 and ABCG1 transport free cholesterol to apoA-I and HDL, respectively, and ACAT converts it to its acyl ester which is stored in lipid droplets. 5α-Epo, 7α-OH, and cholesterol are comparable ACAT substrates, whereas the toxic oxysterols, 5β-Epo, 7β-OH, and 7-ketocholesterol are very poor substrates (*30*). Also, 7-ketocholesterol is a poor substrate for the ABCA1 pathway and even inhibits cholesterol efflux (*27*, *81*, *82*). Oxysterol-treated cells are also associated with adaptive effects found in cholesterol-loaded cells. These effects include the formation of myelin-like figures enriched in free sterol, phosphatidylcholine, and sphingomyelin (*21*), sterol crystals (*22*), free sterols accumulating in isolated plasma membrane fractions (*27*), and steryl esters (*15*, *83*). Free cholesterol induces apoptosis in macrophages when the protective pathways involving ACAT and HDL mediated cholesterol efflux are compromised (*23*−*26*, *73*, *84*). Tabas and associates have investigated free cholesterol-induced apoptosis in macrophages and have generated a biophysical model in which the enrichment of the ER with free cholesterol results in decreased membrane fluidity and decreased activity of the sarcoplasmic−endoplasmic reticulum calcium ATPase (*23*−*26*). The activity of this protein is conformationally regulated and is inhibited in membranes where free cholesterol increases membrane order. They speculate that this biophysical model links excess free cholesterol and the unfolded protein response which appears to be central to the induction of apoptosis in free cholesterol loaded macrophages that occurs in advanced atherosclerotic lesions (*25*, *26*). Recent studies indicated that 7-ketocholesterol, 7β-OH, and 25-OH induce apoptosis in smooth muscle cells by a mechanism that is similar to that of free cholesterol-induced apoptosis in macrophages (*11*). Thus, the underlying mechanism for oxysterol-induced apoptosis in smooth muscle cells may be through alteration of the biophysical properties of the ER membranes. However, in macrophages, free cholesterol and 7-ketocholesterol induce apoptosis by different mechanisms (*25*). 7-Ketocholesterol, 5β-Epo, 7β-OH, and 25-OH induce apoptosis by a mitochondrial death pathway and involves the uptake of extracellular calcium (*12*, *14*), activation of calcium signaling pathways (*12*, *13*, *15*), and the induction of oxidative stress (e.g., activation of leukocyte NADPH oxidase that is found both in monocyte/macrophages and endothelial cells) (*9*, *19*, *20*). The effect of 7-ketocholesterol on the biophysical properties of the plasma membrane has been suggested for increased cellular calcium mediated by the transient receptor potential calcium channel 1 (*12*) and for the inhibition of apoA-I mediated cholesterol efflux (*27*). In cells, sterol chemical structure has been demonstrated to affect compositional and biochemical properties thought to be associated with membrane rafts (*42*, *57*−*59*, *85*). Epidermal growth factor (EGF) signal transduction is a raft-associated process (*86*) that has been demonstrated to be differentially affected by the structure of different oxysterols (*87*). Akt/protein kinase B signaling (*16*), NADPH oxidase activation (*20*), and channel mediated calcium uptake (*12*) have been implicated in oxysterol-mediated apoptosis, and each of these process may be affected by altering membrane cholesterol levels and/or alteration of membrane structure (*88*−*90*). Thus, at least part of the apoptotic effects of oxysterols must occur by the accumulation of excess cellular unesterified oxysterols that can affect the membrane biophysical properties and physiologic function of both cholesterol-rich membranes, i.e., plasma membrane rafts, and the normally cholesterol-poor membranes, e.g., ER, of the rest of the cell.

REFERENCES

1. Bjorkhem, I., and Diczfalusy, U. (2002) Oxysterols: friends, foes, or just fellow passengers? *Arterioscler. Thromb. Vasc. Biol. 22*, 734−742.
2. Olkkonen, V. M., and Lehto, M. (2004) Oxysterols and oxysterol binding proteins: role in lipid metabolism and atherosclerosis, *Ann. Med. 36*, 562−572.
3. Jessup, W., Wilson, P., Gaus, K., and Kritharides, L. (2002) Oxidized lipoproteins and macrophages, *Vasc. Pharmacol. 38*, 239−248.
4. Massey, J. B. (2006) Membrane and protein interactions of oxysterols, *Curr. Opin. Lipidol. 17*, 296−301.
5. Ory, D. S. (2004) Nuclear receptor signaling in the control of cholesterol homeostasis: have the orphans found a home? *Circ. Res. 95*, 660−770.

6. Wang, P. Y., Weng, J., and Anderson, R. G. (2005) OSBP is a cholesterol-regulated scaffolding protein in control of ERK activation, *Science 307*, 1472−1476.
7. Im, Y. J., Raychaudhuri, S., Prinz, W. A., and Hurley, J. H. (2005) Structural mechanism for sterol sensing and transport by OSBP-related proteins, *Nature 437*, 154−158.
8. O'Callaghan, Y. C., Woods, J. A., and O'Brien, N. M. (2001) Comparative study of the cytotoxicity and apoptosis-inducing potential of commonly occurring oxysterols, *Cell Biol. Toxicol. 17*, 127−137.
9. Lemaire-Ewing, S., Prunet, C., Montange, T., Vejux, A., Berthier, A., Bessede, G., Corcos, L., Gambert, P., Neel, D., and Lizard, G. (2005) Comparison of the cytotoxic, pro-oxidant and pro-inflammatory characteristics of different oxysterols, *Cell Biol. Toxicol. 21*, 97−114.
10. Rimner, A., Al Makdessi, S., Sweidan, H., Wischhusen, J., Rabenstein, B., Shatat, K., Mayer, P., and Spyridopoulos, I. (2005) Relevance and mechanism of oxysterol stereospecifity in coronary artery disease, *Free Radic. Biol. Med. 38*, 535−544.
11. Pedruzzi, E., Guichard, C., Ollivier, V., Driss, F., Fay, M., Prunet, C., Marie, J. C., Pouzet, C., Samadi, M., Elbim, C., O'Dowd, Y., Bens, M., Vandewalle, A., Gougerot-Pocidalo, M. A., Lizard, G., and Ogier-Denis, E. (2004) NAD(P)H oxidase Nox-4 mediates 7-ketocholesterol-induced endoplasmic reticulum stress and apoptosis in human aortic smooth muscle cells, *Mol. Cell Biol. 24*, 10703−10717.
12. Berthier, A., Lemaire-Ewing, S., Prunet, C., Monier, S., Athias, A., Bessede, G., Pais de Barros, J. P., Laubriet, A., Gambert, P., Lizard, G., and Neel, D. (2004) Involvement of a calcium-dependent dephosphorylation of BAD associated with the localization of Trpc-1 within lipid rafts in 7-ketocholesterol-induced THP-1 cell apoptosis, *Cell Death Differ. 11*, 897−905.
13. Berthier, A., Lemaire-Ewing, S., Prunet, C., Montange, T., Vejux, A., Pais de Barros, J. P., Monier, S., Gambert, P., Lizard, G., and Neel, D. (2005) 7-Ketocholesterol-induced apoptosis. Involvement of several pro-apoptotic but also anti-apoptotic calcium-dependent transduction pathways, *FEBS J. 272*, 3093−3104.
14. Ryan, L., O'Callaghan, Y. C., and O'Brien, N. M. (2006) Involvement of calcium in 7β -hydroxycholesterol and cholesterol-5β,6β-epoxide induced apoptosis, *Int. J. Toxicol. 25*, 35−39.
15. Freeman, N. E., Rusinol, A. E., Linton, M., Hachey, D. L., Fazio, S., Sinensky, M. S., and Thewke, D. (2005) Acyl-coenzyme A:cholesterol acyltransferase promotes oxidized LDL/oxysterol-induced apoptosis in macrophages, *J. Lipid Res. 46*, 1933−1943.
16. Rusinol, A. E., Thewke, D., Liu, J., Freeman, N., Panini, S. R., and Sinensky, M. S. (2004) AKT/protein kinase B regulation of BCL family members during oxysterol-induced apoptosis, *J. Biol. Chem. 279*, 1392−1399.
17. Ryan, L., O'Callaghan, Y. C., and O'Brien, N. M. (2005) The role of the mitochondria in apoptosis induced by 7β-hydroxycholesterol and cholesterol-5β,6β-epoxide, *Br. J. Nutr. 94*, 519−525.
18. Prunet, C., Lemaire-Ewing, S., Menetrier, F., Neel, D., and Lizard, G. (2005) Activation of caspase-3-dependent and -independent pathways during 7-ketocholesterol- and 7β-hydroxycholesterol-induced cell death: a morphological and biochemical study, *J. Biochem. Mol. Toxicol. 19*, 311−326.
19. Ryan, L., O'Callaghan, Y. C., and O'Brien, N. M. (2004) Generation of an oxidative stress precedes caspase activation during 7β-hydroxycholesterol-induced apoptosis in U937 cells, *J. Biochem. Mol. Toxicol. 18*, 50−59.
20. Rosenblat, M., and Aviram, M. (2002) Oxysterol-induced activation of macrophage NADPH-oxidase enhances cell-mediated oxidation of LDL in the atherosclerotic apolipoprotein E deficient mouse: inhibitory role for vitamin E, *Atherosclerosis 160*, 69−80.
21. Vejux, A., Kahn, E., Dumas, D., Bessede, G., Menetrier, F., Athias, A., Riedinger, J. M., Frouin, F., Stoltz, J. F., Ogier-Denis, E., Todd-Pokropek, A., and Lizard, G. (2005) 7-Ketocholesterol favors lipid accumulation and colocalizes with Nile Red positive cytoplasmic structures formed during 7-ketocholesterol-induced apoptosis: analysis by flow cytometry, FRET biphoton spectral imaging microscopy, and subcellular fractionation, *Cytometry A 64*, 87−100.
22. Geng, Y. J., Phillips, J. E., Mason, R. P., and Casscells, S. W. (2003) Cholesterol crystallization and macrophage apoptosis: implication for atherosclerotic plaque instability and rupture, *Biochem. Pharmacol. 66*, 1485−1492.
23. Feng, B., Yao, P. M., Li, Y., Devlin, C. M., Zhang, D., Harding, H. P., Sweeney, M., Rong, J. X., Kuriakose, G., Fisher, E. A., Marks, A. R., Ron, D., and Tabas, I. (2003) The endoplasmic reticulum is the site of cholesterol-induced cytotoxicity in macrophages, *Nat. Cell Biol. 5*, 781−92.
24. Li, Y., Ge, M., Ciani, L., Kuriakose, G., Westover, E. J., Dura, M., Covey, D. F., Freed, J. H., Maxfield, F. R., Lytton, J., and Tabas, I. (2004) Enrichment of endoplasmic reticulum with cholesterol inhibits sarcoplasmic-endoplasmic reticulum calcium ATPase-2b activity in parallel with increased order of membrane lipids: implications for depletion of endoplasmic reticulum calcium stores and apoptosis in cholesterol-loaded macrophages, *J. Biol. Chem. 279*, 37030−37039.
25. Tabas, I. (2004) Apoptosis and plaque destabilization in atherosclerosis: the role of macrophage apoptosis induced by cholesterol, *Cell Death Differ. 11 Suppl. 1*, S12−16.
26. Maxfield, F. R., and Tabas, I. (2005) Role of cholesterol and lipid organization in disease, *Nature 438*, 612−621.
27. Gaus, K., Kritharides, L., Schmitz, G., Boettcher, A., Drobnik, W., Langmann, T., Quinn, C. M., Death, A., Dean, R. T., and Jessup, W. (2004) Apolipoprotein A-1 interaction with plasma membrane lipid rafts controls cholesterol export from macrophages, *FASEB J. 18*, 574−576.
28. Burger, K., Gimpl, G., and Fahrenholz, F. (2000) Regulation of receptor function by cholesterol, *Cell Mol. Life Sci. 57*, 1577−1592.
29. Radhakrishnan, A., Sun, L. P., Kwon, H. J., Brown, M. S., and Goldstein, J. L. (2004) Direct binding of cholesterol to the purified membrane region of SCAP: mechanism for a sterol-sensing domain, *Mol. Cell. 5*, 259−268.
30. Zhang, Y., Yu, C., Liu, J., Spencer, T. A., Chang, C. C., and Chang, T. Y. (2003) Cholesterol is superior to 7-ketocholesterol or 7 alpha-hydroxycholesterol as an allosteric activator for acyl-coenzyme A:cholesterol acyltransferase 1, *J. Biol. Chem. 278*, 11642−11647.
31. Liu, J., Chang, C. C., Westover, E. J., Covey, D. F., and Chang, T. Y. (2005) Investigating the allosterism of acyl-CoA:cholesterol acyltransferase (ACAT) by using various sterols: in vitro and intact cell studies, *Biochem. J. 391*, 389−397.
32. Simons, K., and Vaz, W. L. (2004) Model systems, lipid rafts, and cell membranes, *Annu. Rev. Biophys. Biomol. Struct. 33*, 269−295.
33. London, E. (2005) How principles of domain formation in model membranes may explain ambiguities concerning lipid raft formation in cells, *Biochim. Biophys. Acta 1746*, 203−220.
34. Pike, L. J. (2004) Lipid rafts: heterogeneity on the high seas, *Biochem. J. 378*, 281−292.
35. Xu, X., and London, E. (2000) The effect of sterol structure on membrane lipid domains reveals how cholesterol can induce lipid domain formation, *Biochemistry 39*, 843−849.
36. Xu, X., Bittman, R., Duportail, G., Heissler, D., Vilcheze, C., and London, E. (2001) Effect of the structure of natural sterols and sphingolipids on the formation of ordered sphingolipid/sterol domains (rafts). Comparison of cholesterol to plant, fungal, and disease-associated sterols and comparison of sphingomyelin, cerebrosides, and ceramide, *J. Biol. Chem. 276*, 33540−33546.
37. Wenz, J. J., and Barrantes, F. J. (2003) Steroid structural requirements for stabilizing or disrupting lipid domains, *Biochemistry 42*, 14267−14276.
38. Li, X. M., Momsen, M. M., Brockman, H. L., and Brown, R. E. (2003) Sterol structure and sphingomyelin acyl chain length modulate lateral packing elasticity and detergent solubility in model membranes, *Biophys. J. 85*, 3788−3801.
39. Wang, J., Megha, and London, E. (2004) Relationship between sterol/steroid structure and participation in ordered lipid domains (lipid rafts): implications for lipid raft structure and function, *Biochemistry 43*, 1010−1018.
40. Bacia, K., Schwille, P., and Kurzchalia, T. (2005) Sterol structure determines the separation of phases and the curvature of the liquid-ordered phase in model membranes, *Proc. Natl. Acad. Sci. U.S.A. 102*, 3272−3277.
41. Beattie, M. E., Veatch, S. L., Stottrup, B. L., and Keller, S. L. (2005) Sterol structure determines miscibility versus melting transitions in lipid vesicles, *Biophys. J. 89*, 1760−1768.
42. Vainio, S., Jansen, M., Koivusalo, M., Rog, T., Karttunen, M., Vattulainen, I., and Ikonen, E. (2006) Significance of sterol structural specificity: Desmosterol cannot replace cholesterol in lipid rafts, *J. Biol. Chem. 281*, 348−355.

43. Stottrup, B. L., and Keller, S. L. (2006) Phase behavior of lipid monolayers containing DPPC and cholesterol analogs, *Biophys. J. 90*, 3176−3183.
44. Barenholz, Y. (2004) Sphingomyelin and cholesterol: from membrane biophysics and rafts to potential medical applications, Subcell. *Biochem. 37*, 167−215.
45. Gallay, J., de Kruijff, B., and Demel, R. A. (1984) Sterol-phospholipid interactions in model membranes. Effect of polar group substitutions in the cholesterol side-chain at C20 and C22, *Biochim. Biophys. Acta. 769*, 96−104.
46. Theunissen, J. J., Jackson, R. L., Kempen, H. J., and Demel, R. A. (1986) Membrane properties of oxysterols. Interfacial orientation, influence on membrane permeability and redistribution between membranes, *Biochim. Biophys. Acta. 860*, 66−74.
47. Verhagen, J. C., ter Braake, P., Teunissen, J., van Ginkel, G., and Sevanian, A. (1996) Physical effects of biologically formed cholesterol oxidation products on lipid membranes investigated with fluorescence depolarization spectroscopy and electron spin resonance, *J. Lipid Res. 37*, 1488−1502.
48. Massey, J. B., and Pownall, H. J. (2005) The polar nature of 7-ketocholesterol determines its location within membrane domains and the kinetics of membrane microsolubilization by apolipoprotein A-I, *Biochemistry 44*, 10423−10433.
49. Kan, C. C., Yan, J., and Bittman, R. (1992) Rates of spontaneous exchange of synthetic radiolabeled sterols between lipid vesicles, *Biochemistry. 31*, 1866−1874.
50. Lange, Y., Ye, J., and Strebel, F. (1995) Movement of 25-hydroxycholesterol from the plasma membrane to the rough endoplasmic reticulum in cultured hepatoma cells, *J. Lipid Res. 36*, 1092−1097.
51. Meaney, S., Bodin, K., Diczfalusy, U., and Bjorkhem, I. (2002) On the rate of translocation in vitro and kinetics in vivo of the major oxysterols in human circulation: critical importance of the position of the oxygen function, *J. Lipid Res. 43*, 2130−2135.
52. Phillips, J. E., Geng, Y. J., and Mason, R. P. (2001) 7-Ketocholesterol forms crystalline domains in model membranes and murine aortic smooth muscle cells, *Atherosclerosis 159*, 125−35.
53. Kauffman, J. M., Westerman, P. W., and Carey, M. C. (2000) Fluorocholesterols, in contrast to hydroxycholesterols, exhibit interfacial properties similar to cholesterol, *J. Lipid Res. 41*, 991−1003.
54. Pownall, H. J., Massey, J. B., Kusserow, S. K., and Gotto, A. M., Jr. (1979) Kinetics of lipid-protein interactions: effect of cholesterol on the association of human plasma high-density apolipoprotein A-I with L-α-dimyristoylphosphatidylcholine, *Biochemistry 20*, 574−9.
55. Massey, J. B., and Pownall, H. J. (2005) Role of oxysterol structure on the microdomain-induced microsolubilization of phospholipid membranes by apolipoprotein A-I, *Biochemistry 44*, 14376−14384.
56. Janowski, B. A., Grogan, M. J., Jones, S. A., Wisely, G. B., Kliewer, S. A., Corey, E. J., and Mangelsdorf, D. J. (1999) Structural requirements of ligands for the oxysterol liver X receptors LXRα and LXR*β*, *Proc. Natl. Acad. Sci. U.S.A. 96*, 266−271.
57. Westover, E. J., Covey, D. F., Brockman, H. L., Brown, R. E., and Pike, L. J. (2003) Cholesterol depletion results in site-specific increases in epidermal growth factor receptor phosphorylation due to membrane level effects. Studies with cholesterol enantiomers, *J. Biol. Chem. 278*, 51125−51133.
58. Campbell, S., Gaus, K., Bittman, R., Jessup, W., Crowe, S., and Mak, J. (2004) The raft-promoting property of virion-associated cholesterol, but not the presence of virion-associated Brij 98 rafts, is a determinant of human immunodeficiency virus type 1 infectivity, *J. Virol. 78*, 10556−10565.
59. Romanenko, V. G., Rothblat, G. H., and Levitan, I. (2004) Sensitivity of volume-regulated anion current to cholesterol structural analogues, *J. Gen. Physiol. 123*, 77−87.
60. King, S. R., Matassa, A. A., White, E. K., Walsh, L. P., Jo, Y., Rao, R. M., Stocco, D. M., and Reyland, M. E. (2004) Oxysterols regulate expression of the steroidogenic acute regulatory protein, *J. Mol. Endocrinol. 32*, 507−517.
61. Ahyayauch, H., Larijani, B., Alonso, A., and Goni, F. M. (2006) Detergent solubilization of phosphatidylcholine bilayers in the fluid state: Influence of the acyl chain structure, *Biochim. Biophys. Acta. 1758*, 190−196.
62. Massey, J. B. (2001) Interaction of ceramides with phosphatidylcholine, sphingomyelin and sphingomyelin/cholesterol bilayers, *Biochim. Biophys. Acta. 1510*, 167−184.
63. Parasassi, T., Di Stefano, M., Loiero, M., Ravagnan, G., and Gratton, E. (1994) Cholesterol modifies water concentration and dynamics in phospholipid bilayers: a fluorescence study using Laurdan probe, *Biophys. J. 66*, 763−768.
64. Lichtenberg, D., Goni, F. M., Heerklotz, H. (2005) Detergent-resistant membranes should not be identified with membrane rafts, *Trends Biochem. Sci. 30*, 430−436.
65. Sot, J., Bagatolli, L. A., Goni, F. M., and Alonso, A. (2006) Detergent-resistant, ceramide-enriched domains in sphingomyelin/ceramide bilayers, *Biophys. J. 90*, 903−914.
66. McKeone, B. J., Pownall, H. J., and Massey, J. B. (1986) Ether phosphatidylcholines: comparison of miscibility with ester phosphatidylcholines and sphingomyelin, vesicle fusion, and association with apolipoprotein A-I, *Biochemistry 25*, 7711−7716.
67. de Almeida, R. F., Fedorov, A., Prieto, M. (2003) Sphingomyelin/phosphatidylcholine/cholesterol phase diagram: boundaries and composition of lipid rafts, *Biophys. J. 85*, 2406−2416.
68. Scherfeld, D., Kahya, N., and Schwille, P. (2003) Lipid dynamics and domain formation in model membranes composed of ternary mixtures of unsaturated and saturated phosphatidylcholines and cholesterol, *Biophys. J. 85*, 3758−3768.
69. Veatch, S. L., Polozov, I. V., Gawrisch, K., and Keller, S. L. (2004) Liquid domains in vesicles investigated by NMR and fluorescence microscopy, *Biophys. J. 86*, 2910−2922.
70. Lange, Y., Ye, J., and Steck, T. L. (2004) How cholesterol homeostasis is regulated by plasma membrane cholesterol in excess of phospholipids, *Proc. Natl. Acad. Sci. U.S.A. 101*, 11664−11667.
71. Lange, Y., Ye, J., and Steck, T. L. (2005) Activation of membrane cholesterol by displacement from phospholipids, *J. Biol. Chem. 280*, 36126−36131.
72. Qin, C., Nagao, T., Grosheva, I., Maxfield, F. R., and Pierini, L. M. (2006) Elevated plasma membrane cholesterol content alters macrophage signaling and function, *Arterioscler. Thromb. Vasc. Biol. 26*, 372−378.
73. Kellner-Weibel, G., Luke, S. J., and Rothblat, G. H. (2003) Cytotoxic cellular cholesterol is selectively removed by apoA-I via ABCA1, *Atherosclerosis 171*, 235−243.
74. Smondyrev, A. M., and Berkowitz, M. L. (2001) Effects of oxygenated sterol on phospholipid bilayer properties: a molecular dynamics simulation, *Chem. Phys. Lipids 112*, 31−39.
75. Xiang, T. X., and Anderson, B. D. (2002) A computer simulation of functional group contributions to free energy in water and a DPPC lipid bilayer, *Biophys. J. 82*, 2052−2066.
76. Nagle, J. F., and Tristram-Nagle, S. (2000) Structure of lipid bilayers, *Biochim. Biophys. Acta 1469*, 159−195.
77. Harroun, T. A., Katsaras, J., and Wassall, S. R. (2006) Cholesterol hydroxyl group is found to reside in the center of a polyunsaturated lipid membrane, *Biochemistry 45*, 1227−1233.
78. Scheidt, H. A., Muller, P., Herrmann, A., and Huster, D. (2003) The potential of fluorescent and spin-labeled steroid analogs to mimic natural cholesterol, *J. Biol. Chem. 278*, 45563−45569.
79. Pulfer, M. K., and Murphy, R. C. (2004) Formation of biologically active oxysterols during ozonolysis of cholesterol present in lung surfactant, *J. Biol. Chem. 279*, 26331−26338.
80. Oram, J. F. (2003) HDL apolipoproteins and ABCA1: partners in the removal of excess cellular cholesterol, *Arterioscler. Thromb. Vasc. Biol. 23*, 720−727.
81. Gelissen, I. C., Rye, K. A., Brown, A. J., Dean, R. T., and Jessup, W. (1999) Oxysterol efflux from macrophage foam cells: the essential role of acceptor phospholipid, *J. Lipid Res. 40*, 1636−1646.
82. Gaus, K., Dean, R. T., Kritharides, L., and Jessup, W. (2001) Inhibition of cholesterol efflux by 7-ketocholesterol: comparison between cells, plasma membrane vesicles, and liposomes as cholesterol donors, *Biochemistry 40*, 13002−13014.
83. Brown, A. J., Mander, E. L., Gelissen, I. C., Kritharides, L., Dean, R. T., and Jessup, W. (2000) Cholesterol and oxysterol metabolism and subcellular distribution in macrophage foam cells. Accumulation of oxidized esters in lysosomes, *J. Lipid Res. 41*, 226−237.
84. Feng, B., and Tabas, I. (2002) ABCA1-mediated cholesterol efflux is defective in free cholesterol-loaded macrophages. Mechanism involves enhanced ABCA1 degradation in a process requiring full NPC1 activity, *J. Biol. Chem. 277*, 43271−43280.
85. Keller, R. K., Arnold, T. P., and Fliesler, S, J. (2004) Formation of 7-dehydrocholesterol-containing membrane rafts in vitro and in vivo, with relevance to the Smith-Lemli-Opitz syndrome, *J. Lipid Res. 45*, 347−355.

86. Pike, L. J. (2005) Growth factor receptors, lipid rafts and caveolae: an evolving story, *Biochim. Biophys. Acta. 1746*, 260−273.
87. Pike, L. J., and Miller, J. M. (1998) Cholesterol depletion delocalizes phosphatidylinositol bisphosphate and inhibits hormone-stimulated phosphatidylinositol turnover, *J. Biol. Chem. 273*, 22298−22304.
88. Zhuang, L., Kim, J., Adam, R. M., Solomon, K. R., and Freeman, M. R. (2005) Cholesterol targeting alters lipid raft composition and cell survival in prostate cancer cells and xenografts, *J. Clin. Invest. 115*, 959−968.
89. Vilhardt, F., and van Deurs, B. (2004) The phagocyte NADPH oxidase depends on cholesterol-enriched membrane microdomains for assembly, *EMBO J. 23*, 739−748.
90. Zhang, A. Y., Yi, F., Zhang, G., Gulbins, E., and Li, P. L. (2006) Lipid raft clustering and redox signaling platform formation in coronary arterial endothelial cells, *Hypertension 47*, 74−80.

BI060540U